FILE

INTERNAL DOCUMENT 137

I.O.S.

A SEISMIC REFRACTION AND REFLECTION STUDY OF CONTINENT-OCEAN TRANSITION BENEATH THE NORTH BISCAY MARGIN

F. Avedik, A.L. Camus, A. Ginzburg
L. Montadert, D.G. Roberts and R.B. Whitmarsh

Internal Document No. 137

July 1981

NATURAL ENVIRONMENT RESEARCH COUNCIL
INSTITUTE OF OCEANOGRAPHIC SCIENCES

INSTITUTE OF OCEANOGRAPHIC SCIENCES

Wormley, Godalming,
Surrey GU8 5UB
(042-879-4141)

(Director: Dr. A. S. Laughton)

Bidston Observatory,
Birkenhead,
Merseyside L43 7RA
(051-653-8633)
(Assistant Director: Dr. D. E. Cartwright)

Crossway,
Taunton,
Somerset TA1 2DW
(0823-86211)
(Assistant Director: M. J. Tucker)

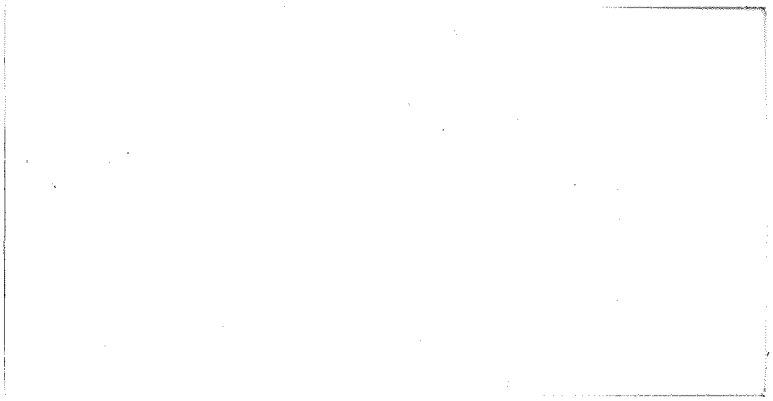

A SEISMIC REFRACTION AND REFLECTION STUDY OF CONTINENT-OCEAN TRANSITION BENEATH THE NORTH BISCAY MARGIN

F. Avedik, A.L. Camus, A. Ginzburg
L. Montadert, D.G. Roberts and R.B. Whitmarsh

Internal Document No. 137

July 1981

Work carried out under contract to the Department of Energy

Institute of Oceanographic Sciences,
Brook Road,
Wormley,
Godalming,
Surrey. GU8 5UB

INTRODUCTION

Theoretical models of lithospheric extension, as well as the geological consequences of such extension in the form of rifted cratonic basins and of passive continental margins, have attracted considerable recent interest. In the European area, examples of rifted cratonic basins include the North Sea (Ziegler, 1978 and this volume) and the adjacent margins of the North Atlantic Ocean. It has become clear that extension may also occur in strike slip and convergent settings (Bally & Snelson, 1979), and examples include the Western Mediterranean (Biju-Duval et al., 1977), the Pannonian Basin (Royden & Sclater, 1981) and the Great Basin (Profett, 1977). The occurrence of crustal extension, expressed by rifting, in these different geological settings emphasises that very little is known of the mechanisms producing the rifting process, including its initiation, which cause the profound changes in crustal structure revealed by attenuation and ultimately by the formation of a spreading ocean basin.

Several innovative theoretical models (McKenzie, 1978; Royden et al., 1980; Royden and Keen, 1980; Sclater & Christie, 1981; Turcotte, 1981) have proposed mechanisms for lithospheric extension and have attempted to evaluate quantitatively the mechanical and thermal consequences of each model in terms of histories of margin and basin subsidence. These models may have a potential practical value in predicting the thermal history and thus the degree of hydrocarbon maturity in sedimentary basins formed in response to a lithospheric extension (Royden & Keen, 1980; Royden et al., 1980; Sclater & Christie, 1980). However, a rigorous description of the deep crustal structure beneath a cratonic sedimentary basin or a passive continental margin that would provide sufficient data to quantify the extension in order to constrain these models has been lacking as has a comprehensive study of the geological and thermal history of basins that have evolved in response to lithospheric extension.

In this paper, we present some of the results of a detail seismic refraction and reflection study of the northern or Armorican margin of the Bay of Biscay. The study examined the deep crustal structure

of the rifted and attenuated continental crust and of the transition to the adjoining oceanic crust. It is believed to be the first time such a detailed seismic description of a rifted passive margin has been obtained. A comprehensive discussion of the seismic data and their interpretation will be published elsewhere (Ginzburg et al., in preparation).

REGIONAL STRUCTURE OF NORTHERN BISCAY

The continental margin in the Southwestern Approaches to the English Channel (Figure 1) consists of a broad shelf, a relatively steep slope and a broad rise that merges imperceptibly with the Biscay Abyssal Plain. The shelf is underlain by the NE-SW trending Western Approaches Basin which seems to intersect the margin. Further north, the Cornubian High separates the Western Approaches Basin from the Celtic Sea Basin (Montadert et al., 1979; Roberts et al., 1981).

Beneath the slope and rise multichannel seismic reflection profiles show that the margin consists of thin Tertiary and Cretaceous sediments that overlie a series of large tilted and rotated fault blocks. Rifting apparently took place in Late Jurassic-Early Cretaceous time in a pre-existing marine basin and was completed by Late Aptian time (Montadert, Roberts et al., 1977; Montadert et al., 1979). The overall tectonic style consists of tilted and rotated fault blocks whose downthrow is consistently down toward the ocean. The pattern of faults is probably en-echelon or anastomosing. Many of the fault blocks are bounded by listric normal faults (Fig. 2a) with throws of up to 3000 m. The listric faults flatten out with depth close to the top of a sub-horizontal group of reflectors called 'S' (Fig. 2b). Comparison with early refraction data suggested that this reflector corresponded to the boundary between a 4.9 and 6.3 $km.sec^{-1}$ layer (Avedik & Howard, 1979). De Charpal et al. (1979) and Montadert et al. (1979) interpreted the 6.3 $km.sec^{-1}$ refractor as the boundary between the upper brittle and the lower ductile continental crust. Refraction data on the shelf (Holder & Bott, 1971) suggested that the Moho shoaled from 25 km beneath the shelf break to 12 km near the continent-ocean transition where, from the available refraction data, the observed ductile crust was estimated to be only 3 km

in thickness. These early results showed that the observed thinning of the crust could not be fully explained by the extension of 10-15% in the upper crust and resulted in the suggestion that the lower ductile had thinned by a greater amount (De Charpal et al., 1978; Montadert et al., 1979). The drill, dredge and reflection data suggested that at the end of rifting a system of half-graben about 2.5 km below sea level existed adjacent to the continent-ocean transition (Montadert, Roberts et al., 1977, 1979). After rifting regional subsidence took place in response to cooling of the lithosphere of which the continental crustal part had been thinned during the rifting process. This interpretation of attenuation, although based on good quality multichannel seismic data, was dependent on earlier refraction profiles whose directions are now known to cross underlying fault blocks.

EXPERIMENTAL DESIGN

In June 1979, a number of single ship refraction profiles and two-ship reflection and refraction profiles were occupied on the margin. The purpose of the experiment was to define the variation in the deep structure of the continental crust from beneath the shelf, to define the continent-ocean transition and to examine the relative amounts of thinning in the upper and lower parts of the crust. The experiment was also designed to examine the width and nature of the transition from continental to oceanic crust.

The study was carried out in two parts. During the first phase refraction profiles were shot by RRS Shackleton using the Pop-Up Bottom Seismographs (PUBS) of the Institute of Oceanographic Sciences (Kirk et al., in preparation) and the Ocean Bottom Seismographs (OBS) of the Centre Océanologique de Bretagne (Avedik et al., 1978) along the lines shown in Figure 3a. The study area, some 30 km west of the region studied in detail around Site 400A (Montadert et al., 1979), was selected to avoid complications that might be posed by the prominent uplift associated with Late Eocene-Oligocene shearing in the vicinity of the Trevelyan escarpment. Line 1 was situated on the oceanic crust and line 2 on the presumed thinned continental crust. As far as was possible these lines were oriented parallel

to the continent-ocean transition and in the case of line 2, parallel to the strike of the tilted blocks. An additional unpublished reversed refraction line (Fig. 3a) situated on the ocean crust south of line 1 and made with PUBS (Discovery Station 6737-6739) was reinterpreted and incorporated in the study. Line 3 consisted of a long refraction profile from the ocean crust to the shelf encompassing the continent-ocean transition and the progressive change from attenuated crust to thick crust beneath the shelf. PUBS and OBS were deployed at various points along the line to give a series of overlapping reversed profiles. The energy source used along lines 1, 2 and 3 was a 4 x 1000 in^3 airgun array. Profile 4 along the shelf was unreversed and was shot using explosive charges of up to 600 lbs. It was intended to use explosives along line 3 but this was not possible for reasons beyond our control.

During the second phase of the experiment (Figure 3b) RRS Shackleton and the RV Résolution of the Institut Français du Pétrole occupied a series of two-ship multichannel seismic reflection profiles. RRS Shackleton acted as the shooting ship using a 4 x 1000 in^3 airgun array and RV Résolution acted as receiving ship using a 2.4 km 48-trace streamer. Relative positioning was maintained using a PULSE-8 shore based radio-navigation system (accuracy $\pm$ 25 m) and radar. Shot breaks were transmitted from Shackleton to Résolution using a time break transmitter. The following types of two-ship profile were made. Along refraction lines 1 and 2 on either side of the continent-ocean transition, two-ship expanding spread profiles were made to ranges of 35 km. In addition, along both these lines and part of line 3, 30 km fixed offset profiles were made; 30 km was chosen as the offset from a preliminary Moho depth estimate to ensure that only Pn arrivals would be obtained as first arrivals. Five kilometre fixed offset reflection profiles were also made along the whole of line 3 and line 4. Conventional 24-fold 48-trace reflection profiles were also obtained along all refraction profiles by R.V. Résolution. Bathymetric and gravity data were acquired on all profiles by RRS Shackleton.

To aid the seismic and gravity modelling, a multichannel seismic reflection profile extending from the continental shelf to the ocean crust with a recording length of 12 seconds (IOS line CM-14) was

migrated by the Institut Français du Pétrole. We discuss below interpretation of the expanding spread (Camus, 1980) and refraction data. The fixed offset data have been discussed in part by Camus (1981) and will be presented in Ginzburg et al., (in preparation).

EXPANDING SPREAD SEISMIC PROFILES

The principles of two-ship expanding spread seismic reflection profiling have been discussed by Stoffa and Buhl (1979) and a detailed discussion of the way in which our data was processed can be found in Camus (1980).

In this experiment, RRS Shackleton acted as shooting ship using a 4 x 1000 in^3 airgun and R.V. Résolution as receiving ship using a 48-trace (2400 m) streamer. The time interval between shots was 80 seconds, resulting in a shot to receiver spacing increment of 400 m at a speed over the ground of 5 knots maintained by each ship. The position of the expanding spread profiles (ESP) on either side of the continent-ocean transition is shown in Figure 3b. The recorded data were subjected to wave number and frequency filtering prior to 6-fold stacking to ensure maximum enhancement of signal.

Interpretation of the expanding spread data has been made with reference to individual shots (48-traces per shot), as well as to the stacked section.

Individual shots in expanding spread seismic profiles

The slope(s) and intercept(s) of refracted arrivals were measured for each individual shot. This method was used to take advantage of the precision with which slopes could be measured. The multiple measurements of velocities along the line were used to assess variations in apparent velocity within a given layer. Examples of some traces displayed using different reduction velocities are shown in Figure 4.

The range of apparent velocities and intercept times are tabulated below.

TABLE 1

Apparent velocity and intercept data (individual shots) expanding spread lines 1 and 2

Line 1 (oceanic crust)				Line 2 (thinned continental crust)			
Velocity ($km.sec^{-1}$)		Intercept (secs)		Velocity ($km.sec^{-1}$)		Intercept (secs)	
From	To	From	To	From	To	From	To
2.0				2.0			
3.65	3.8	6.4	6.75	3.5	3.7	6.3	6.4
4.4	5.3	7.6	8.4	4.5	4.7	7.2	7.3
6.5	6.8	8.5	8.8	6.1	6.7	8.1	8.4
7.3	7.8	9	9.3	8.1	8.7	8.7	8.7

In the line 1 (ocean crust) data, the 6.5-6.8 $km.sec^{-1}$ arrivals have come from the top of the oceanic layer 3 and the 7.3-7.8 $km.sec^{-1}$ arrivals are from the Moho.

In the line 2 (thinned continental crust) data, the 4.5 to 4.7 $km.sec^{-1}$ velocity is a refraction from the top of the tilted blocks. The 6.1-6.7 $km.sec^{-1}$ refractor is the top of the crystalline basement within the tilted blocks and the 8.1-8.7 $km.sec^{-1}$ refractor is the Moho.

In comparing the two lines, the scatter of the intercepts is greater on line 1 situated on the oceanic crust. Although the scatter may be due in part to the existence of strong velocity gradients within the oceanic basement, some of the scatter of velocities and intercepts on both lines probably results from the oceanic basement topography on line 1 or the tilted blocks on line 2. For example, a dip of 10^{o} on a 8.2 $km.sec^{-1}$ refractor will reduce the apparent velocity to 7.55 $km.sec^{-1}$.

Stacked expanding spread data (Figure 5a)

Results from the expanding spread profile along line 2 are shown in Figure 5a. Each ESP was shot twice, with the two ships

first approaching and then going away from each other. Intercept times were measured on both sides of the stacked sections to give averaged apparent refraction velocities and intercept times (Camus, 1980).

The results calculated assuming horizontal layering are given in Table II.

TABLE II

Line 1 (oceanic crust) from expanding spread data.

Velocity ($km.sec^{-1}$)	Velocity Accuracy	Intercept (secs)	Depth (km)
1.51			
2.35		4.95	4.6
3.5	±5%	6.65	6.1
4.8	±8%	7.8	7.95
6.7	±8%	8.85	10.2
7.8		9.4	12.5

Line 2 (thinned continental crust) from expanding spread data

Velocity ($km.sec^{-1}$)	Velocity Accuracy	Intercept (secs)	Depth (km)
1.51			
2.4		4.7	4.52
3.5	±5%	6.4	6.1
4.6	±8%	7.3	7.4
6.4	±8%	8.25	9.2
8.2		8.9	11.2

Using these results, travel-time curves for lines 1 and 2 have been calculated and both the refracted and reflected branches are in good agreement with the observed travel-time data (Figure 5b) (Camus, 1980).

SEISMIC REFRACTION PROFILES

Seismic refraction profiles were occupied along lines 1, 2, 3 and 4 using PUBS and OBS. Data were recorded in analogue form in the PUBS and by pulse-coded modulation on the OBS. A 4 x 1000 in^3 airgun array

firing every two minutes at 2000 psi was used as the sound source on lines 1, 2 and 3. Line 4 was shot using explosive charges of 25 lbs for the near shots and 300 or 600 lbs for the far shots. Ranges were computed for each trace for the PUBS data and every 15 shots for the OBS by computer modelling of water-wave travel-times. Sound speeds in the sea down to 2000m were obtained from velocimeter data (IOS unpublished data) and to greater depths from Fenner and Bucca (1971).

The PUBS data were digitised at 100 samples per second and the digitized data were plotted as filtered reduced travel-time record sections. Because of the low signal to noise ratio, particularly at ranges greater than 15 km from the PUBS, three trace running averages were applied to the PUBS traces and the averaged sections were used for picking arrival times. The OBS data were displayed as unreduced, unaveraged variable area record sections on which apparent velocities, but not arrival onsets, could be read with confidence.

In interpreting the data, a preliminary model was constructed based on estimates of true velocities from updip and downdip apparent velocities and from depths calculated by standard velocity intercept methods. This model was then input into a two-dimensional ray tracing programme (Makris, 1977) which was used to develop the final models. A timing correction was applied to all the arrival times to extend the ray paths to the sea-surface vertically above the PUBS and OBS. The correction was based on a refraction velocity of 8 $km.s^{-1}$. Errors in this assumption will only be significant for arrivals from the uppermost crust not studied in detail here. For Station 6739, amplitudes were modelled using synthetic seismograms computed by the Fuchs and Muller (1971) reflectivity method to estimate gradients within the oceanic crust (Figure 6). In addition, the models were constrained by thickness and interval velocity data for the upper sedimentary layers computed from the multichannel seismic lines and, where available, from the expanding spread refraction data.

Refraction line 1 (oceanic crust)

An OBS was deployed at each end of line 1 and a PUBS in the centre.

Although refracted arrivals do not persist over distances greater than 35-40 km from the OBS, a reversed refraction profile was thus obtained (Figure 3a, 7). Calculated velocities are 2.35 and 3.32 km.s^{-1} (sediments), 4.44 km.s^{-1} (layer 2), 6.6 km.s^{-1} (layer 3) and 7.9 km.s^{-1} (upper mantle). These velocities are in good agreement with those calculated for lines 6737 and 6739 some 30 km south of line 1. The 4.44 km.sec^{-1} refractor corresponds to the 3.5 and 4.8 km.sec^{-1} refractors observed on the unreversed ESP line 1 (Table II). The existence of velocity gradients was deduced from the 6737 and 6739 data and is confirmed on line 1 by the concentration of energy near the 6.7-6.9 km.sec^{-1} crossover distance in the PUBS data. The thicknesses of the various layers are: sediments 2.6 to 3.0 kms, layer 2 1.6km, layer 3 varied from 2.4 km in the west to 2 km in the east (Figure 7). The model calculations were based on the arrival times and apparent velocities obtained for the PUBS data because of the poor quality of the OBS data on this line.

Refraction line 2 (thinned continental crust)

Two PUBS deployed at each end of the line (Figure 3a) yielded record sections which have been used to calculate the model in Figure 8. The velocities in this model are 3.43 km.s^{-1} for the second sediment layer, 4.52 km.s^{-1} (Palaeozoic or Mesozoic? sediments), 6.2 km.sec^{-1} (crystalline basement) and 8.05 km.s^{-1} (upper mantle). The 6.2 km.s^{-1} layer is 2.5 to 3.0 km thick and dips gently westward as does the Moho. The configuration of the interfaces above the crystalline basement was obtained from the multichannel reflection profiles.

Refraction profile 3

Refraction profile 3 (Figure 3a) extends across the entire margin from the shelf to the Biscay Abyssal Plain. The profile was designed to examine the thinning of the continental crust as well as the transition from thinned continental crust to oceanic crust. The profile connects the two transverse refraction profiles discussed

above and profile 4. Three PUBS and three OBS were deployed along the line (Figure 3a). Although it was originally intended to use explosive charges to obtain good arrivals at long ranges, this proved impossible and the airgun array was perforce used, thereby severely limiting the quality of the data.

The velocity structure used to constrain the refraction models at the south end of line 3 is derived from the reversed refraction profiles 1 and 2. After allowing for variations in sediment thickness obtained from multichannel seismic profiles along line 3 (lines IFP-3 and IOS CM-14, Figure 3b) all variations in apparent velocity have been attributed to dip variations and not to lateral velocity variations within layers. Each reversed refraction profile between adjacent PUBS or OBS along line 3 was interpreted independently to obtain a section by section model for the whole line.

PUBS 4 was located on oceanic crust at the southern end of line 3 (Figure 3a). The split refraction profile recorded by this PUBS covers the segment of line 3 from just south of line 2 to the southern end of the line. The velocity distribution used in computing the model was that of line 1. The segment of the split profile south of PUBS 4 is shown in Figure 9. Layer 3 apparently thins southward from 3 km to 2.5 km.

The next segment of line 3 was recorded from PUBS 2 situated on thinned continental crust 15 km north of refraction profile 2 (Figure 3a). Readable arrivals were observed to a range of 30 km to the south of PUBS 2 (Figure 10). Four distinct arrivals are present and correspond to the 3.43 $km.s^{-1}$ and 4.52 $km.s^{-1}$ sedimentary layers, the 6.2 $km.s^{-1}$ crystalline basement and the Moho. North of PUBS 2, however, arrivals were recorded only out to a range of 25 km and the Pn arrivals were thus not observed. However, the Pg arrivals define the configuration of the crystalline basement. The velocity distribution used in the models is derived from refraction line 2.

The results of modelling the refraction profiles from PUBS 2 and 4 provide some constraint on the position of the continent-ocean boundary. Modelling of the observations made at PUBS 2, using the velocity distribution calculated for refraction profile 2, gave good agreement

between calculation and observation. However, use of the velocity distribution obtained for line 1 situated on ocean crust did not give good agreement. The converse was found in attempting to apply the results of refraction line 1 to the data obtained at PUBS 2. The discrepancy indicates that a major lateral change in crustal structure, here interpreted as the continent-ocean transition, is present within the region between PUBS 2 and PUBS 4 and probably is located between PUBS 4 and refraction profile 2 (Figure 3a).

The record section south of OBS JULIE (Figure 3a) has been modelled using the results from PUBS 2, refraction line 2, and the multichannel reflection profiles IFP-3 and IOS CM-14. The signal to noise ratio of the record section is low and it is fairly certain that picks at ranges over 50km do not represent the onset of the event. Nonetheless, the model, which is fairly well constrained by the above data shows the progressive thickening of the crust, and particularly the lower crust, towards the shelf (Figure 11). Unfortunately, because of the poor quality of the data, P^* and PIP arrivals could not be identified in the later arrivals so that the position of the discontinuity between the upper and lower crust and its behaviour in relation to the crustal thickening could not be determined.

Refraction profile 4

The refraction profile 4 (Figures 3a, 12) is unreversed and was shot on the shelf across line 3 using explosives. No reflection data were available along this line and there is thus very little control on the depth and attitude of the sedimentary layers. However, a prominent basement high is evident from travel times. To satisfy the observed travel-time of the PmP reflection, it has been necessary to somewhat arbitrarily divide the crust into an upper layer with a velocity gradient from 6.2 $km.s^{-1}$ at the top to 6.4 $km.s^{-1}$ at the base and a lower crustal layer with velocities ranging from 6.4 $km.s^{-1}$ at the top to 6.7 $km.s^{-1}$ at the base.

SURVEY OF THE REFRACTION INTERPRETATION

A summary true-scale section of the distribution of the principal

refracting interfaces along line 3 is shown in Figure 13 together with the positions of the OBS and PUBS. Depths of the interfaces have been interpolated between OBS JULIE on line 3 and line 4 on the shelf. Uncertainties in the data are shown by dashed lines. The continent-ocean transition is inferred to lie within a narrow 8-10km wide zone immediately south of refraction profile 2 from the following three lines of evidence. Firstly, ray trace modelling of crustal structure south of PUBS 4 made using the velocity distribution determined for the thinned continental crust along line 2 does not provide satisfactory agreement with the observed refracted arrivals. This indicates that the transition must occur north of PUBS 4 and south of refraction line 2 and PUBS 2. Secondly, the position of the transition in this region is independently suggested by the marked difference in the velocity gradients observed in the basement along lines 1 and 2. Thirdly, the refracted arrivals observed on the 30 km fixed offset profile recorded along the southern part of line 3 also show a significant change in this region. South of the inferred transition, only mantle arrivals were observed but to the north arrivals from both basement and mantle are present. A distinct zone of about 10km width from which no arrivals were recorded coincides with the transition zone identified from the above data (Camus, 1981).

The composite profile has a number of interesting features which will be noted here and discussed in more detail in the conclusions. Moho depths are very similar on either side of the transition but mantle velocities are different (c.f. 8.05 and 7.9 $km.s^{-1}$). Within the continental crust, the 4.52 $km.s^{-1}$ layer remains relatively constant in thickness in contrast to the underlying crystalline basement which thickens from 3 to 12 km progressively toward the continent.

GRAVITY MODELS

Although the refraction data provided a very good description of the variation in crustal structure across the entire margin, the absence of information on the behaviour of the upper crust/lower crust boundary, as revealed near the foot of the slope by the 'S reflector' on multichannel seismic profiles, was particularly disappointing. As an

alternative approach, an attempt was made to model the observed gravity profile using the results from the refraction experiment.

Initially density boundaries were not introduced within the continental crust in order to test the agreement between calculated and observed free-air gravity anomalies using the refraction data alone. Interfaces were taken directly from the seismic models and the continent-ocean boundary was positioned from the criteria discussed above. Sediment densities were picked from figures in Hamilton (1978), continental crustal densities from the Nafe-Drake (1963) curve, oceanic crustal densities from Christensen and Salisbury (1975) and mantle densities from Christensen (1966). The model was computed using the two-dimensional method of Talwani et al. (1959). The results (Figure 14a) show a substantial discrepancy indicating that greater mass must exist within or beneath the continental crust with respect to the oceanic crust. This excess can be accounted for by lateral density variations in the upper mantle and/or within the lower continental crust. Further modelling showed that the required density variations in the upper mantle violate the refraction data and that more reasonable values do not fully account for the observed mass excess. A third model was computed, using a density interface within the crystalline part of the continental crust. The depth of this interface was arbitrarily chosen to correspond to the 'S reflector'. A small lateral variation in mantle density also needed to be included in the model (Figure 14b). Agreement between calculation and observation is good. In particular, the model supports substantial oceanward thinning of the lower continental crust from 7 km to almost zero at about 100 km from the foot of the slope. Indeed, the possibility that the Moho and the base of the upper crust (S reflector) are coincident cannot be excluded from the gravity interpretation. In marked contrast, the upper part of the crystalline continental crust remains relatively uniform in thickness between the foot of the slope and the continent-ocean transition.

DISCUSSION AND CONCLUSIONS

The results from the seismic refraction study, multichannel seismic reflection profiles and gravity modelling have been combined in the true scale section across the entire north margin of Biscay displayed in Figure 15. The geometry of the fault blocks has been reconstructed from migrated seismic sections (lines IFP-13 and IOS CM-14), subsequently

converted to depth using both interval and refraction velocity data. Depths of the deeper interfaces have been taken from the refraction models. The position of the 'S reflector' is approximate and has been computed from interval velocity data in the sedimentary layers and the 6.2 to 6.4 $km.s^{-1}$ refraction velocity in the crystalline basement.

The section has several features which have an important bearing on the problem of the measurement, as well as the mechanism, of crustal attenuation along rifted margins.

The observed position of the 'S reflector' indicates differential thinning within the crystalline continental crust toward the continent-ocean boundary and the gravity model does not exclude this possibility. The lower crystalline crust thins oceanward near OBS JULIE and to a value near zero close to the continent-ocean transition. In this region, the 'S reflector' observed on seismic profiles may be a complex event arising from the intra-crustal discontinuity and the immediately subjacent Moho. The section indicates that the larger part of the lower crust has been lost. Thinning is also evident in the upper crystalline part of the crust but in contrast it has a global β value of between 2.5 and 3 from the shelf to the continent-ocean transition. Over the region of extreme thinning in the lower crust, the upper crust remains relatively uniform in thickness. A third estimate of extension can be derived from the rotation of the tilted blocks. Using a true-scale section computed from the migrated multichannel seismic profile, the quantity of extension β has been found for the blocks between OBS JULIE and the continent-ocean transition. Values range between 1.1 and 1.45 and are similar to the range of values computed by Chenet et al. (in press) but are significantly lower than values of about 3 found for the tilted blocks by Le Pichon and Sibuet (1981 and this volume).

Estimates of the extension parameter β found by Le Pichon and Sibuet (1980) for the upper crust on the north margin of Biscay have been interpreted by them in terms of the model of uniform extension of the whole lithosphere developed by McKenzie (1978). However, the results of the refraction survey and these calculations indicate that there has been substantially greater thinning of the lower

crust than the upper. The extension parameter derived for the tilted blocks is not representative of the overall extension of the crust as was earlier noted by De Charpal et al., 1979 and Montadert et al. (1979). Indeed, according to our results, the global thinning of the crust (4.8) is much greater than that estimated by Le Pichon and Sibuet (1981).

The difference in the thinning of the upper and lower crust creates an obvious mass balance problem of some importance in extension models. One solution is to invoke rift subsidence as a consequence of a gabbro-eclogite phase transition at the Moho as proposed by Artyushkov and Sobolev (1981). Another hypothesis is to propose that extension of the lithosphere, which perhaps had already been weakened during a previous rifting in Permo-Triassic time, began by brittle failure above and ductile failure below the 'S reflector'. As extension continued, the lower ductile part of the crust became progressively heated and gradually modified by the addition of new mantle that effectively converted the lower crust into a modified upper mantle. The lateral variation in upper mantle density implied by this hypothesis is also suggested by the best-fitting gravity model (Figure 14b). Clearly, more work is required to assess lateral variations in the upper mantle and lower crust in the transition zone. Continued thinning by brittle and ductile flow with contemporaneous conversion of the thinned lower crust took place until the thinned upper crust rested directly on the hot upper mantle. At this stage when the outer part of the rifted margin had subsided by rifting to about 2.0 km (Montadert et al., 1979), the asthensophere might have been able to break through thus causing the initiation of sea-floor spreading.

ACKNOWLEDGEMENTS

We wish to acknowledge support for this study from the UK Department of Energy, the Natural Environment Research Council, the Centre Océanologique de Bretagne, the Institut Français du Pétrole, the Centre Nationale pour l'Exploitation des Océans and the Comité des Etudes Petrolières Marins. The Masters and ships' crews of R.V. Résolution and RRS Shackleton are thanked for their co-operation. The work could not have been done without the help of R.E. Kirk, J.J. Langford, P.R. Miles, S. Smith,

G. Aubert, R. Conogan and R. Paron on RRS Shackleton and M. Cassand on R.V. Résolution. The time break transmitter was kindly loaned by Sociétée Nationale des Pétroles Aquitaine.

REFERENCES

Artyushkov, E.V. and Sobolev, S.F. (1981). Origin of Crustal Subsidence on Passive Margins. Mem. Am Ass. Petrol. Geol. in press.

Avedik, F. & Howard, D. (1979). Preliminary results of a seismic refraction study in the Meriadzek-Trevelyan area, Bay of Biscay. In: Initial Reports Deep Sea Drilling Project, 48, 1015-1023. US Government Printing Office.

Avedik, F., Renard, V., Buisine, D. & Cornic, J-Y. (1978). Ocean bottom refraction seismograph (OBS). Mar. geophys. Res., 3(4), 357-379.

Bally, A.W. & Snelson, S. (1980). Realms of subsidence. Pp 9-94 In: Facts and Principles of World Petroleum Occurrence. Ed. A.D. Miall. Canad. Soc. Petrol. Geol. Mem. 6.

Biju-Duval, B., Dercourt, J. & Pichon, X. Le (1977). From the Tethys Ocean to the Mediterranean Sea: a plate tectonic model of the Western Alpine system, pp 143-164 in Structural History of the Mediterranean Basins. Ed. Biju-Duval, B. & Montadert, L. Editions Technip, Paris.

Camus, A-L. (1980). Campagne Sismique Refraction marge continentale Nord Gascogne. Inst. Français du Pétrole Rept. 28 310, 100 pp.

Camus, A-L. (1981) Campagne Sismique Refraction: analyse des documents 'Distance fixe 30 km'. Institut Français du Pétrole Rept. 28 898, 63 pp.

Charpal, O. de, Guennoc, P., Montadert, L. & Roberts, D.G. (1978). Rifting, crustal attenuation and subsidence in the Bay of Biscay, Nature, 275, 706-711.

Chenet, P.Y., Montadert, L., Gairaud, H. and Roberts, D.G. (1981) in press. Extension rate measurements on the margins of Galicia and North Biscay: consequences for models of passive margin evolution. Mem. Amer. Ass. Petrol. Geol.

Christensen, N.I. and Salisbury, M.H. (1975). Structure and constitution of the lower oceanic crust. Rev. geophys. Space Phys., 13(1), 57-86.

Christensen, N.I. (1966). Elasticity of ultrabasic rocks, J. Geophys. Res., 71, 5921-5931.

Fenner, D.F. & Bucca, P.J. (1971). The sound velocity structure of the North Atlantic Ocean. US Naval Oceanographic Office Informal Report No. 71-13, 86 pp.

Fuchs, K. & Muller, G. (1971). Computation of synthetic seismograms with the reflectivity method and comparison with observations. Geophys. J. Roy. astr. Soc., 23, 417-433.

Hamilton, E.L. (1978). Sound velocity-density relations in sea-floor sediments and rocks, J. Acoust. Soc. Amer., 63, 366-377.

Holder, A.P. & Bott, M.H.P., (1971). Crustal structure in the vicinity of South West England. Geophys. J. Roy. astr. Soc., 23, 465-489.

Kirk, R.E., Langford, J.J. & Whitmarsh, R.B. (in prep.). A functional three-component ocean-bottom seismograph for controlled source and earthquake seismology.

Le Pichon, X & Sibuet, J.C. (1981) - this volume. A model for the passive margins of Biscay.

Le Pichon, X. & Sibuet, J.C. (1981). Passive margins - a model of formation. J. Geophys. Res., 86, 3708-3720.

Makris, J. (1977). Geophysical investigation of the Hellenides. Geophys. Einzelschriften, 34, 1-124.

McKenzie, D.P. (1978). Some remarks on the development of sedimentary basins. Earth Planet Sci. Lett., 40, 25-32.

Montadert, L., Roberts, D.G. et al. (1977). Rifting and subsidence on passive margins in the North East Atlantic. Nature, 268, 305-309.

Montadert, L., Roberts, D.G., Charpal, O. de & Guennoc, P. (1979). Rifting and subsidence of the Northern Continental Margin of the Bay of Biscay in: Initial Reports Deep Sea Drilling Project 48, 1025-1060. US Government Printing Office.

Nafe, J. & Drake, C.L. (1963). Physical properties of marine sediments of the Sea. Volume III Ed: M.N. Hill, Interscience, London pp794-815.

Profett, J.M. (1977). Cenozoic geology of the Yerington district, Nevada and implications for the nature and origin of basin and range faulting. Geol. Soc. Amer. Bull., 88, 247-266.

Roberts, D.G., Masson, D.G., Montadert, L. and Charpal, O. de (1981). Continental Margin from the Porcupine Seabight to the Armorican marginal basin. Pp 455-473 in: Petroleum Geology of the continental shelf of Northwest Europe, Inst. Petroleum, London.

Royden, L. and Sclater, J.G. (1981). The Neogene Intra-Carpathian Basins. Phil. Trans. R. Soc. Lond., A300, 219-222.

Royden, L., Sclater, J.G. and Von Herzen, R.P. (1980). Continental margin subsidence and heat flow: important parameters in the formation of petroleum hydrocarbons. Amer. Ass. Petrl. Geol. Bull., 64, 173-187.

Royden, R. and Keen, C.E. (1980). Rifting process and thermal evolution of the continental margin of Eastern Canada determined from subsidence curves. Earth Planet. Sci. Lett, 51(2), 343-361.

Sclater, J.G. & Christie, P.A.F. (1980). Continental stretching - an explanation of the post Mid-Cretaceous subsidence of the Central North Sea Basin. J. geophys. Res. 85 (37), 3711-3739.

Stoffa, P.L. & Buhl, P. (1979). Two-ship multichannel seismic experiments for deep crustal studies: expanded spread and constant offset profiles. J. geophys. Res., 84 (B), 7645-7660.

Talwani, M., Worzel, J.L. & Landisman, M. (1959). Rapid gravity computations for two-dimensional bodies with application to the Mendocino Submarine Fracture Zone. J. geophys. Res., 64 (1), 49-59.

Turcotte, D.L. (1981) - this volume. Thermal mechanisms of basin formation.

Ziegler, P.A. (1978). Northwestern Europe: Tectonics and basement development. Geologie en Mijnbouw, 57, 589-626.

Ziegler, P.A. (1981) - this volume. Faulting and graben formation in western and central Europe.

FIGURE CAPTIONS

Figure 1) Regional structure of the continental margin of north Biscay (after Roberts et al., 1981).

Figure 2a) An example of a series of prominent tilted and rotated fault blocks bounded by listric normal faults. The blocks contain presumed Jurassic and Early Mesozoic sediments, faulted during the Late Jurassic-Early Cretaceous rifting episode. The position of site 400A is shown (Montadert, Roberts et al., 1979).

b) Seismic profile south of Goban Spur showing the relationship of the 'S reflector' to the tilted blocks (after De Charpal et al., 1979).

Figure 3a) Position of seismic refraction lines in relation to the major structural elements of the margin (after Montadert, Roberts et al., 1979). 1=OBS ISIS, J=OBS JULIE.

b) Position of two-ship expanding spread (ESP), 30 km and 5 km fixed offset profiles in relation to the major structural elements of the margin. Conventional 24-fold 48-trace multichannel single ship profiles were occupied along all offset profiles with the exception of line 4. The position of line IOS CM-14 is also shown.

Figure 4) Expanding spread profile 1: examples of 48-traces per shot data displayed at different reduction velocities (from Camus, 1980).

Figure 5a) Expanding spread profile 2. Vertical scale in 2-way seconds. Horizontal scale in kms.

b) Hodochrone of expanding spread profile 2. Vertical scale in 2-way seconds, horizontal scale in metres.

Figure 6a) Synthetic seismogram of Station 6739 (reduction velocity 8 $km.sec^{-1}$)

b) True amplitude record section (reduction velocity 8 $km.sec^{-1}$) of Station 6739 (for location see Fig. 3a). Hodochrons derived from the model in Fig. 6c.

Figure 6c) Ray trace model of the structure along reversed refraction line 6737-6739.

Figure 7) Ray trace model of refraction profile 1 (oceanic crust) obtained using OBS and PUBS. Velocities are in $km.sec^{-1}$. Horizontal scale in km. For location see Fig. 3a.

Figure 8) Ray trace model of refraction profile 2 (thinned continental crust) obtained using PUBS and OBS. Velocities are in $km.sec^{-1}$.

Figure 9) Ray trace model of reversed segment of line 3 from PUBS-4 to the south situated on oceanic crust. Velocities are in $km.sec^{-1}$. Horizontal scale in km. For location see Fig. 3a.

Figure 10) Ray trace model of reversed segment of line-3 from PUBS-2 to the south on thinned continental crust immediately north of the continent-ocean transition (cf Fig. 9). Velocities are in $km.sec^{-1}$. Horizontal scale in km. For location see Fig. 3a.

Figure 11) Ray trace model of reversed segment of line-3 from OBS JULIE to the southward. Note the progressive deepening of the Moho toward the continent and thickening of the crystalline crust (VP = 6.2 $km.sec^{-1}$). Velocities in $km.sec^{-1}$. Horizontal scale in km. For location see Fig. 3a.

Figure 12) Ray trace model of unreversed line-4 shot on the shelf. Velocities in $km.sec^{-1}$. Horizontal scale in km. For location see Fig. 3a.

Figure 13) Summary true-scale section of refraction results along line-3. No vertical exaggeration. Velocities in $km.sec^{-1}$. Interfaces have been interpolated between OBS JULIE and the shelf. Uncertainties are shown by dashed lines. The continent-ocean transition lies between PUBS-4 and PUBS-2. For location of section see Fig. 3a.

Figure 14a) Calculated (+) and observed (continuous line) free-air gravity profile along line-3. Interfaces have been taken from the summary section in Figure 13, and densities from

various publications (see text). The density model extended far beyond the limits of the figure and was constrained by the whole section in Figure 13. The density contrasts in the upper mantle persisted to 40 km depth.

Figure 14b) Calculated and observed free-air gravity profile along line-3. A density contrast in the crystalline crust at about the level of the 'S reflector' and a lateral variation in mantle density have been used to produce the agreement between calculated and observed anomaly. Otherwise the model is as in Figure 13a. Note the thinning of the lower crust toward the continent-ocean transition. The gravity residuals can probably be explained by a lack of two-dimensionality in the real world. Note the different gravity scale with respect to Fig. 14a.

Figure 15) Summary section across the continental margin of North Biscay incorporating the results of the seismic refraction profile along line-3, migrated 24-fold 48-trace multichannel seismic profiles IPF-3 and IOS CM-14, and the gravity interpretation. For discussion see text.

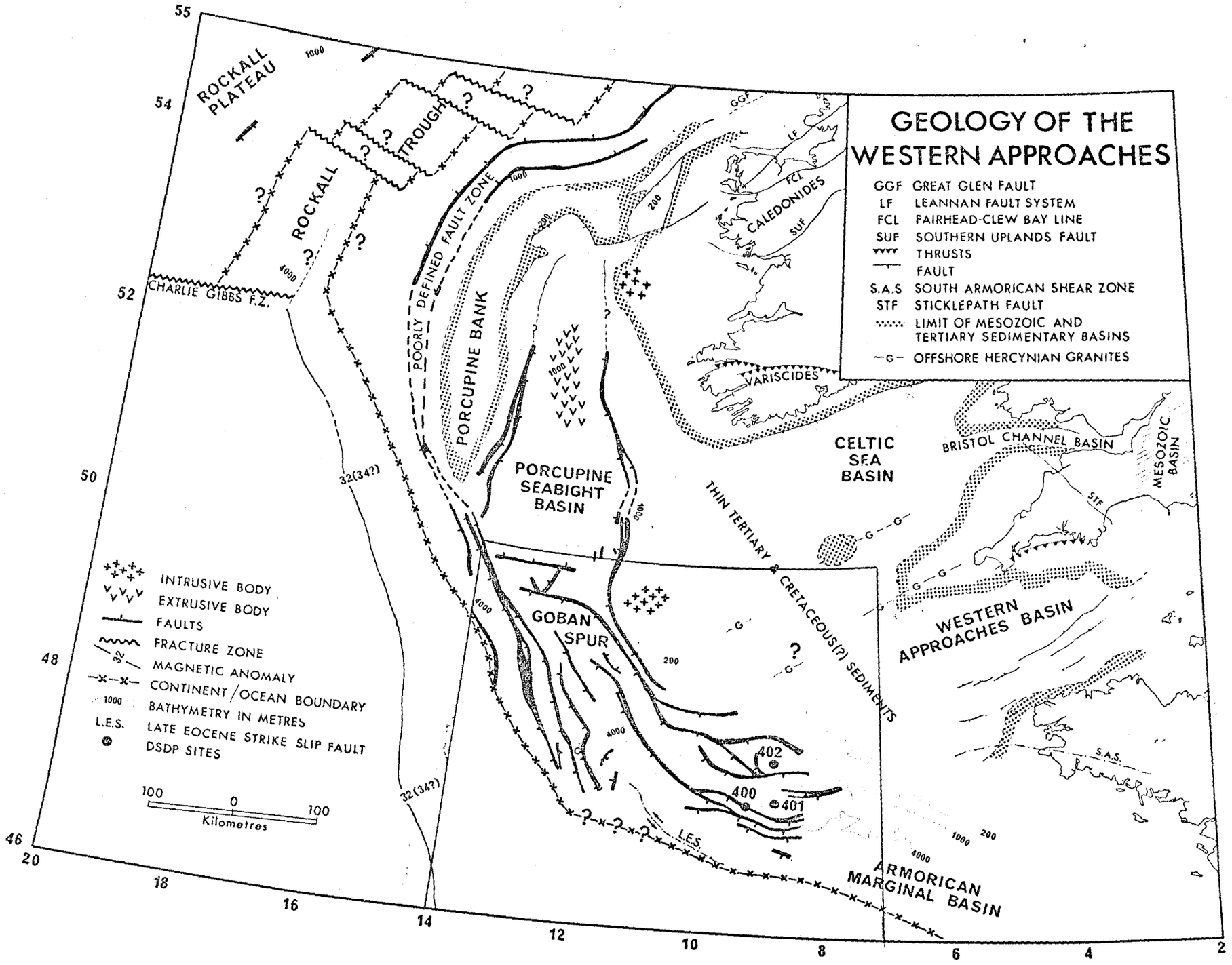
GEOLOGY OF THE WESTERN APPROACHES
GGF GREAT GLEN FAULT
LF LEANNAN FAULT SYSTEM
FCL FAIRHEAD-CLEW BAY LINE
SUF SOUTHERN UPLANDS FAULT
THRUSTS
FAULT
S.A.S SOUTH ARMORICAN SHEAR ZONE
STF STICKLEPATH FAULT
LIMIT OF MESOZOIC AND TERTIARY SEDIMENTARY BASINS
OFFSHORE HERCYNIAN GRANITES
ROCKALL PLATEAU
ROCKALL TROUGH
CHARLIE GIBBS F.Z.
POORLY DEFINED FAULT ZONE
PORCUPINE BANK
PORCUPINE SEABIGHT BASIN
CALEDONIDES
VARISCIDES
CELTIC SEA BASIN
BRISTOL CHANNEL BASIN
MESOZOIC BASIN
THIN TERTIARY & CRETACEOUS(?) SEDIMENTS
GOBAN SPUR
WESTERN APPROACHES BASIN
ARMORICAN MARGINAL BASIN
L.E.S.
32(34?)
INTRUSIVE BODY
EXTRUSIVE BODY
FAULTS
FRACTURE ZONE
MAGNETIC ANOMALY
CONTINENT/OCEAN BOUNDARY
BATHYMETRY IN METRES
LATE EOCENE STRIKE SLIP FAULT
DSDP SITES
100 0 100
Kilometres
400
401
402
55
54
52
50
48
46
20
18
16
14
12
10
8
6
4
2

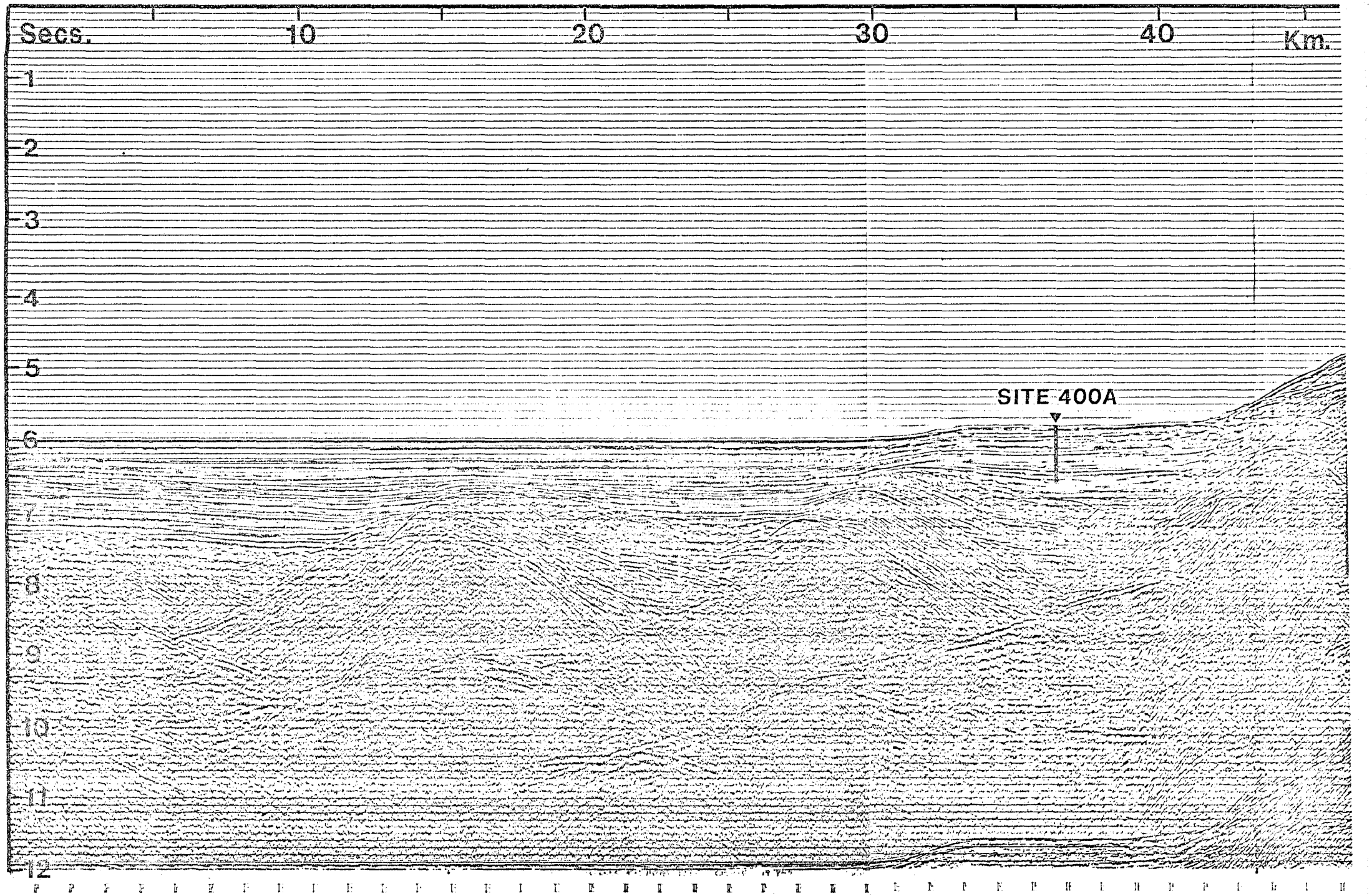
Secs.
10
20
30
40
Km.
1
2
3
4
5
6
7
8
9
10
11
12
SITE 400A

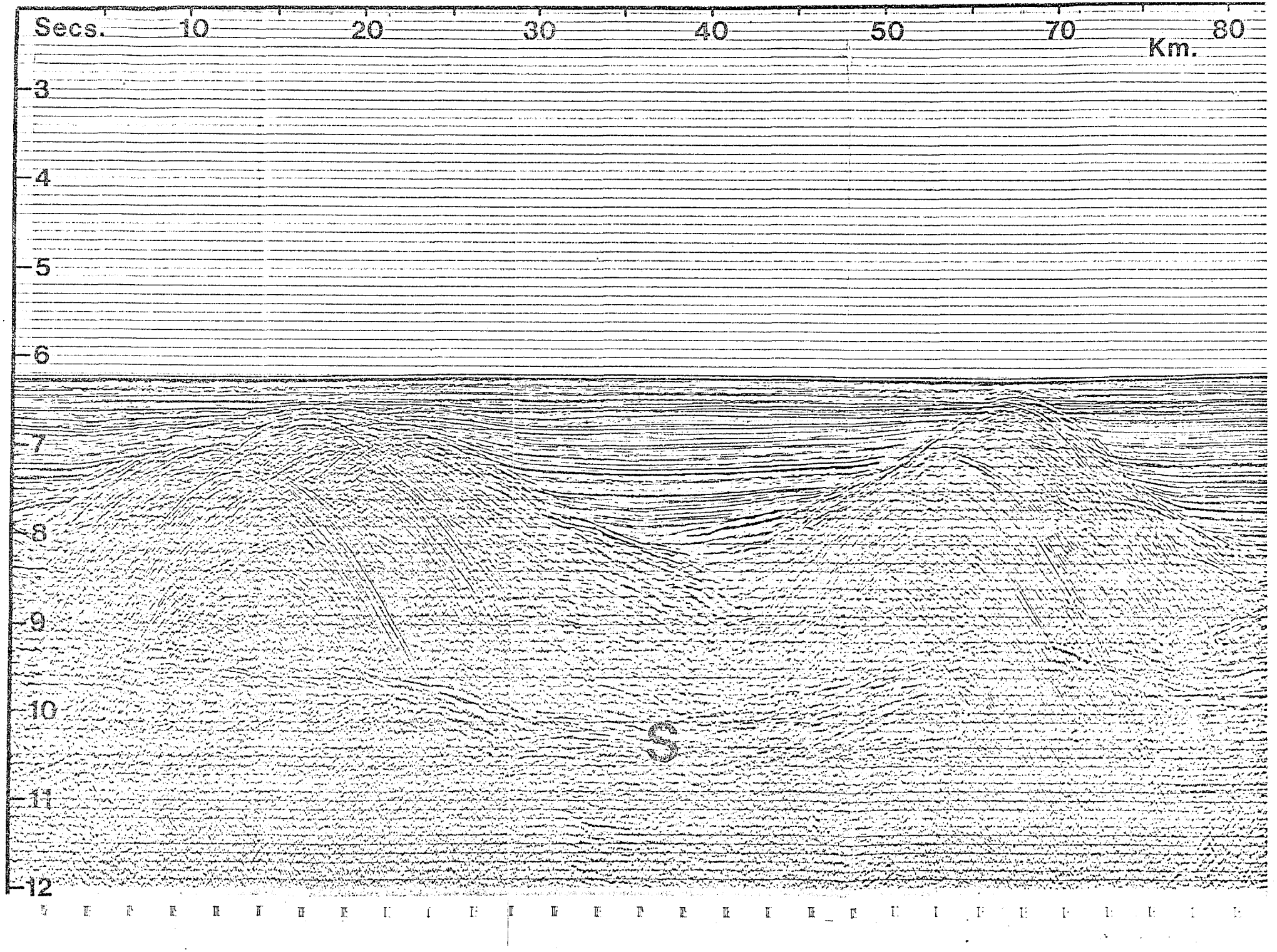
Secs.
10
20
30
40
50
70
80
Km.
3
4
5
6
7
8
9
10
11
12
S

Seismic Study-Biscay
Continental-ocean boundary

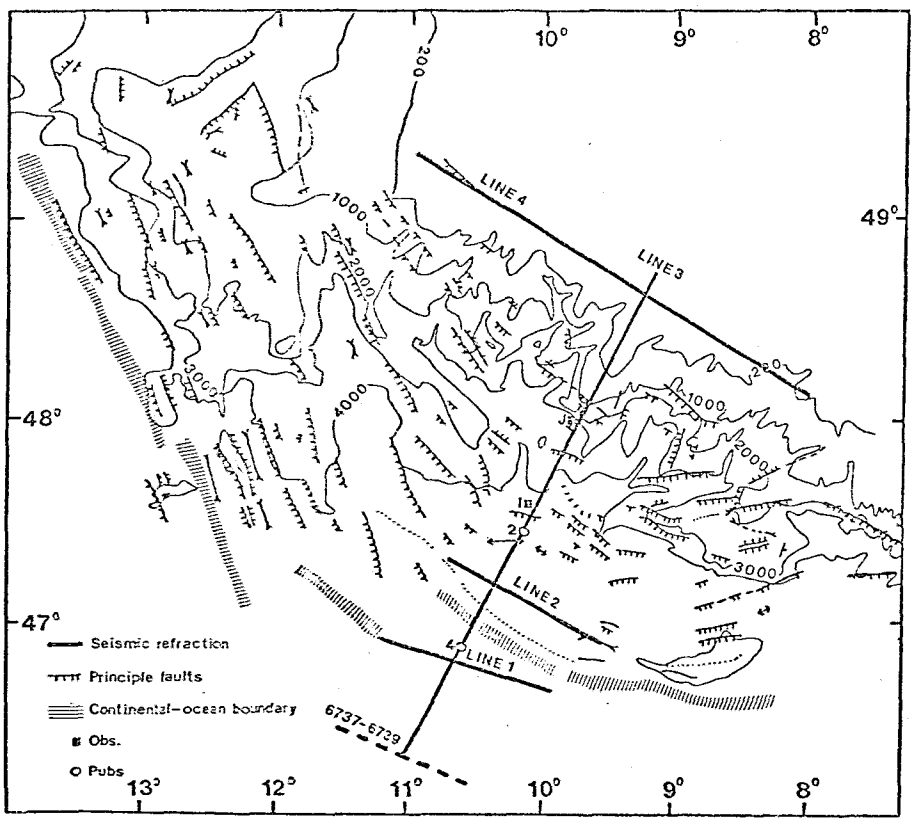

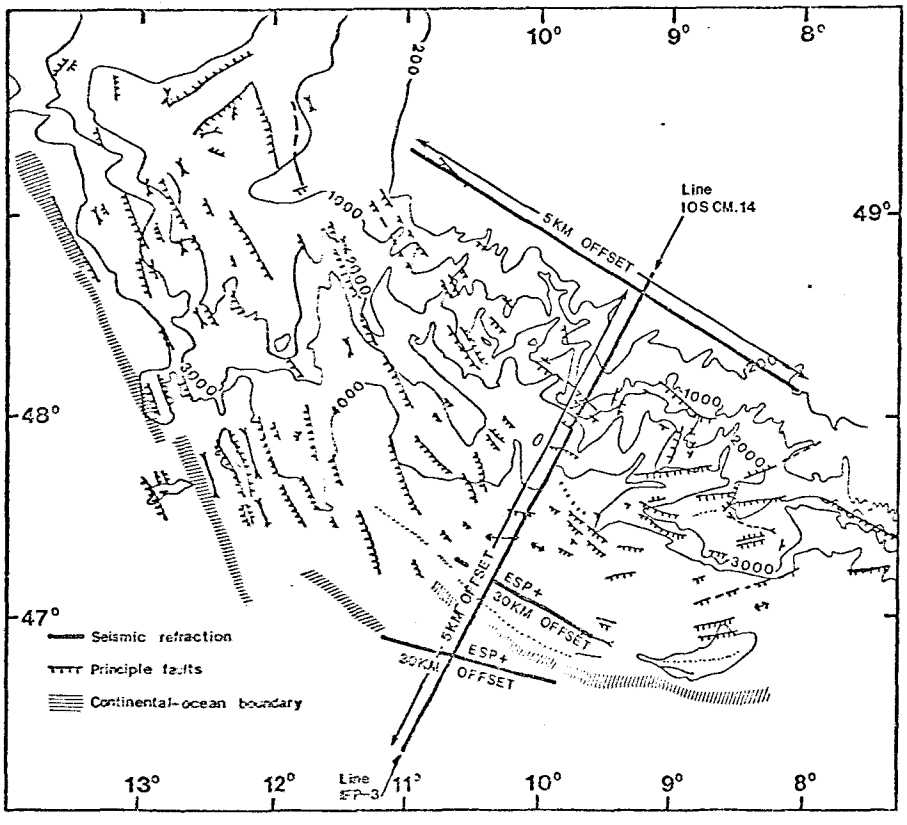

MISE A L'HORIZONTALE DE REFRACTIONS

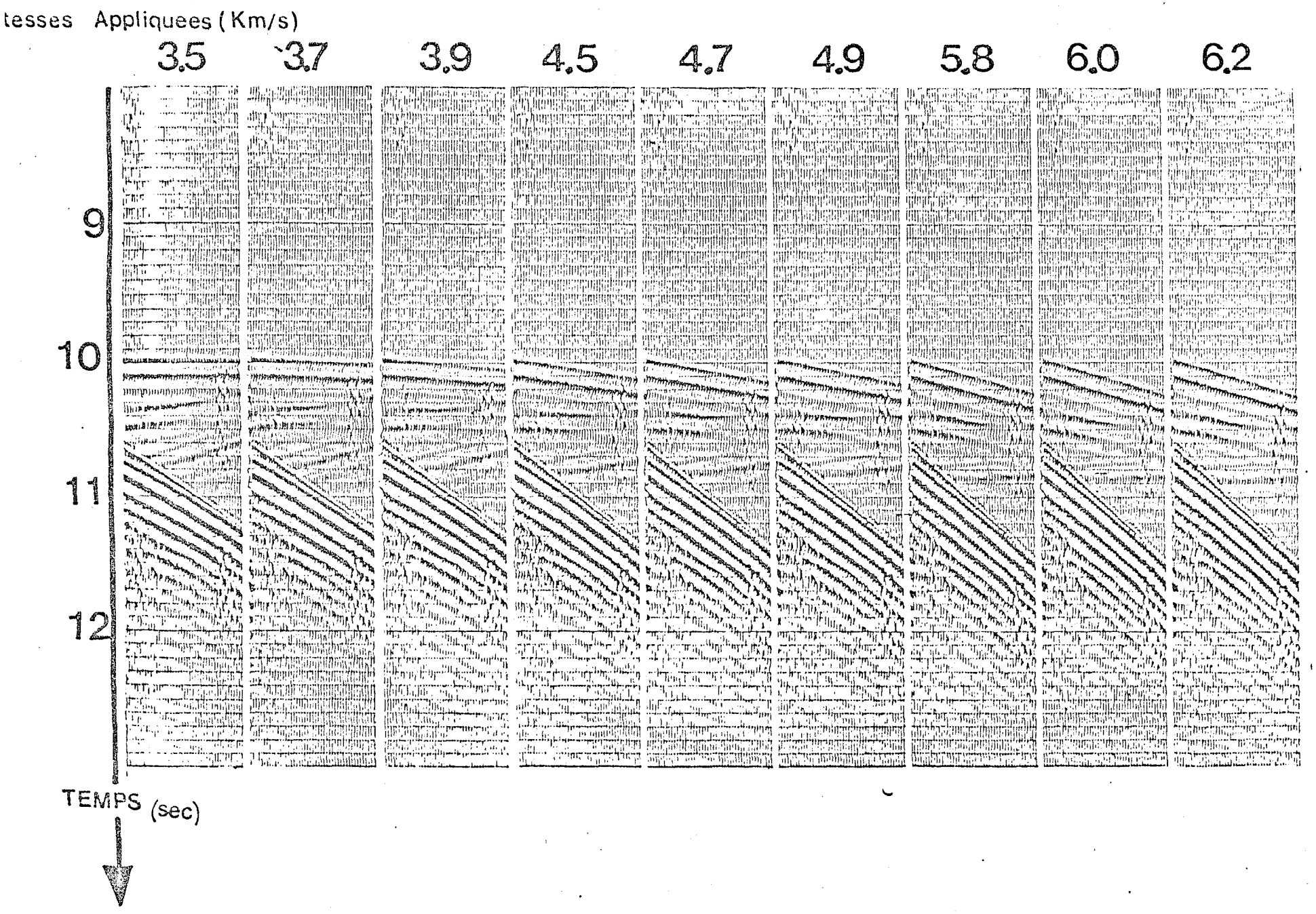

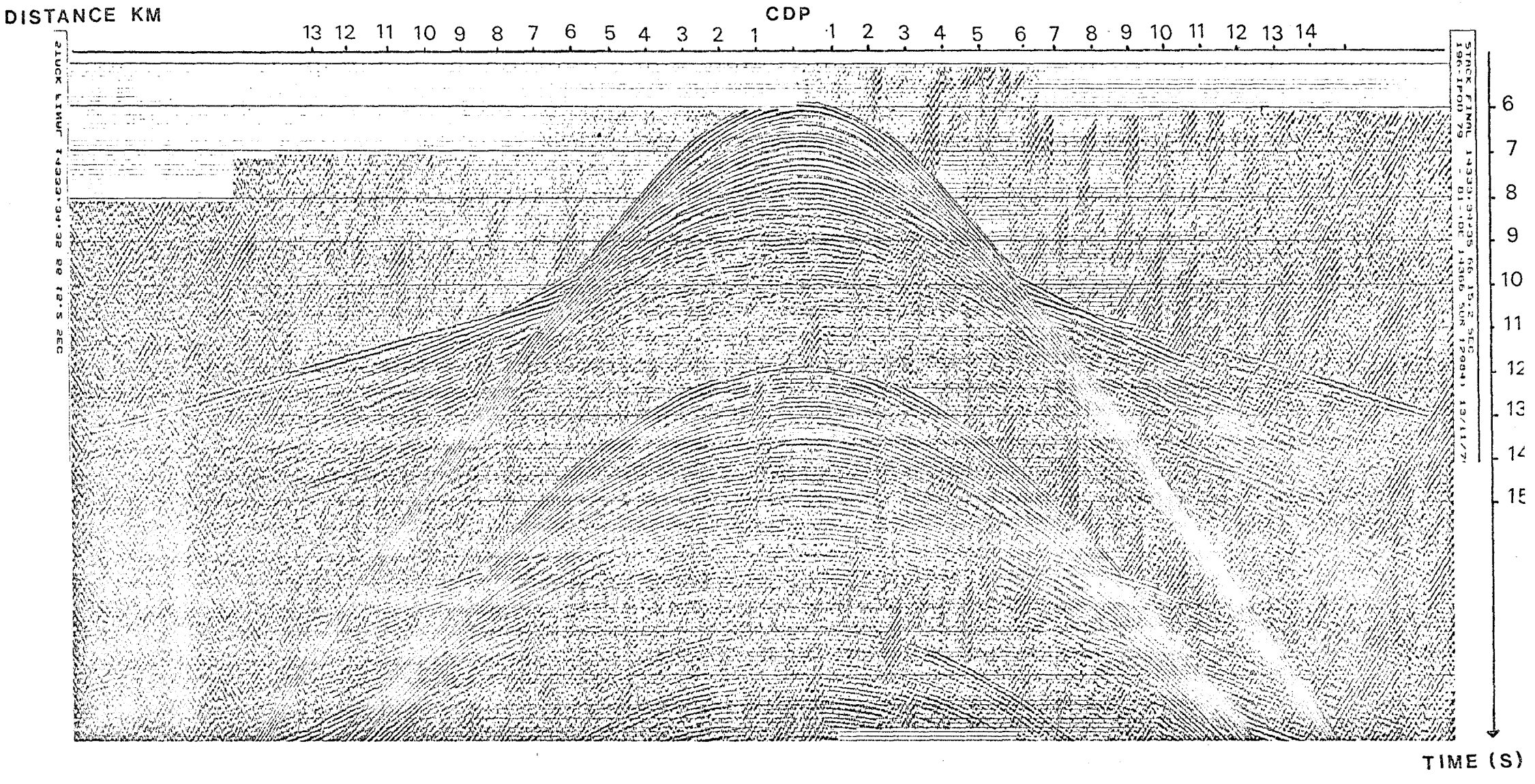
DISTANCE KM
CDP
13 12 11 10 9 8 7 6 5 4 3 2 1
1 2 3 4 5 6 7 8 9 10 11 12 13 14
6
7
8
9
10
11
12
13
14
15
TIME (S)

LINE 2

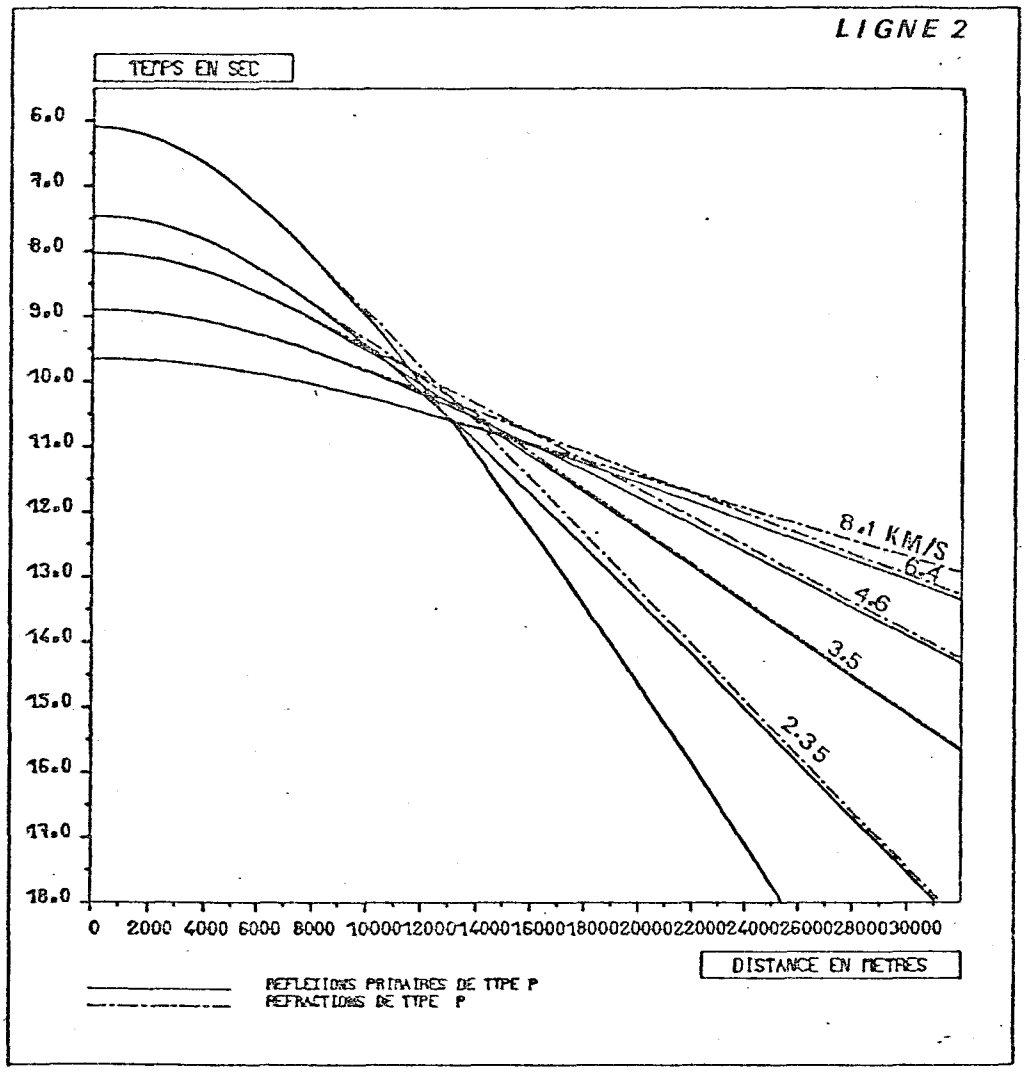
LIGNE 2
TEMPS EN SEC
6.0
7.0
8.0
9.0
10.0
11.0
12.0
13.0
14.0
15.0
16.0
17.0
18.0
0 2000 4000 6000 8000 10000 12000 14000 16000 18000 20000 22000 24000 26000 28000 30000
DISTANCE EN METRES
8.1 KM/S
6.4
4.6
3.5
2.35
REFLEXIONS PRIMAIRES DE TYPE P
REFRACTIONS DE TYPE P

SB

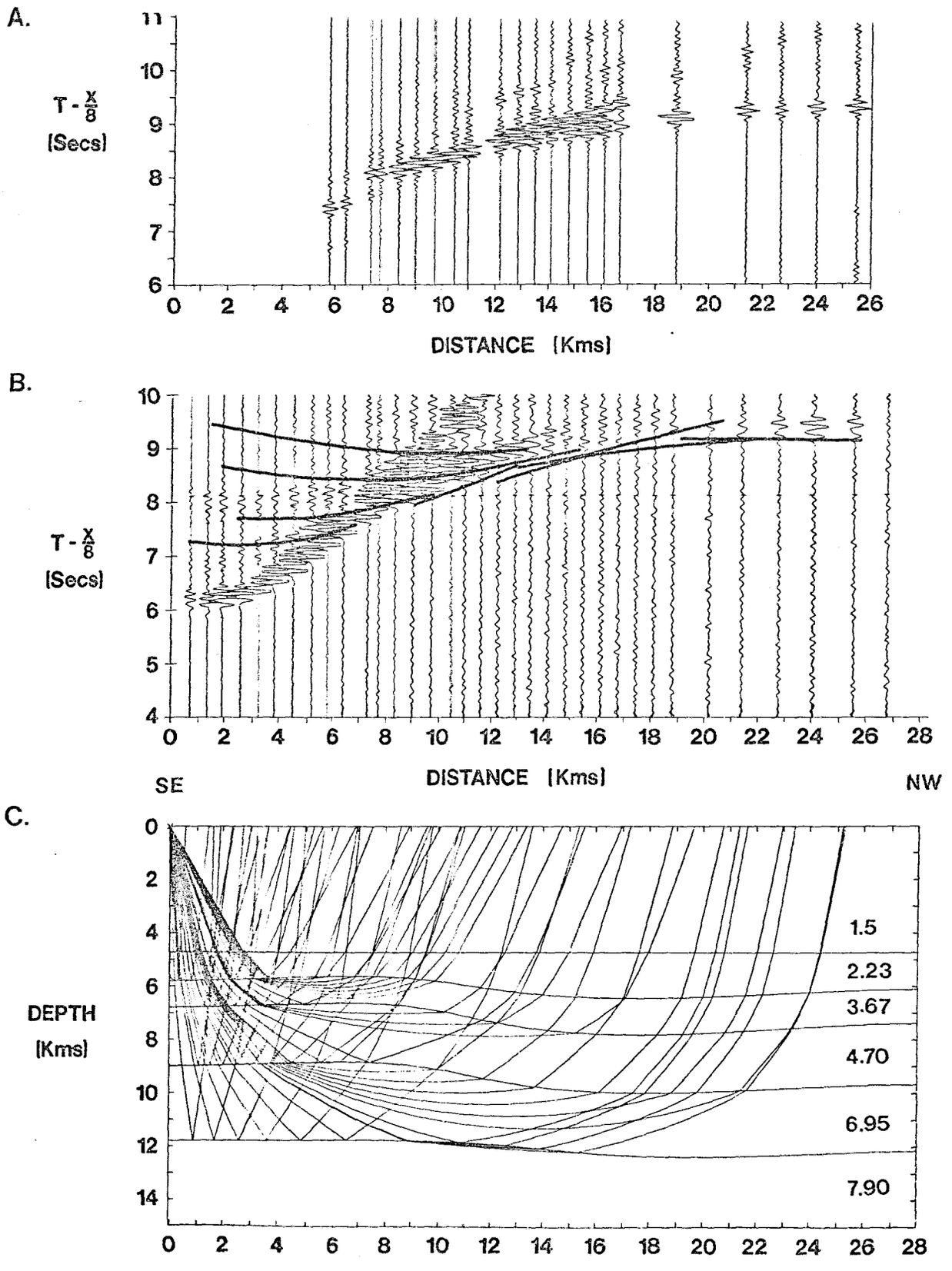
A.
T - X/8
(Secs)
11
10
9
8
7
6
0 2 4 6 8 10 12 14 16 18 20 22 24 26
DISTANCE (Kms)
B.
T - X/8
(Secs)
10
9
8
7
6
5
4
0 2 4 6 8 10 12 14 16 18 20 22 24 26 28
SE
DISTANCE (Kms)
NW
C.
DEPTH
(Kms)
0
2
4
6
8
10
12
14
1.5
2.23
3.67
4.70
6.95
7.90
0 2 4 6 8 10 12 14 16 18 20 22 24 26 28

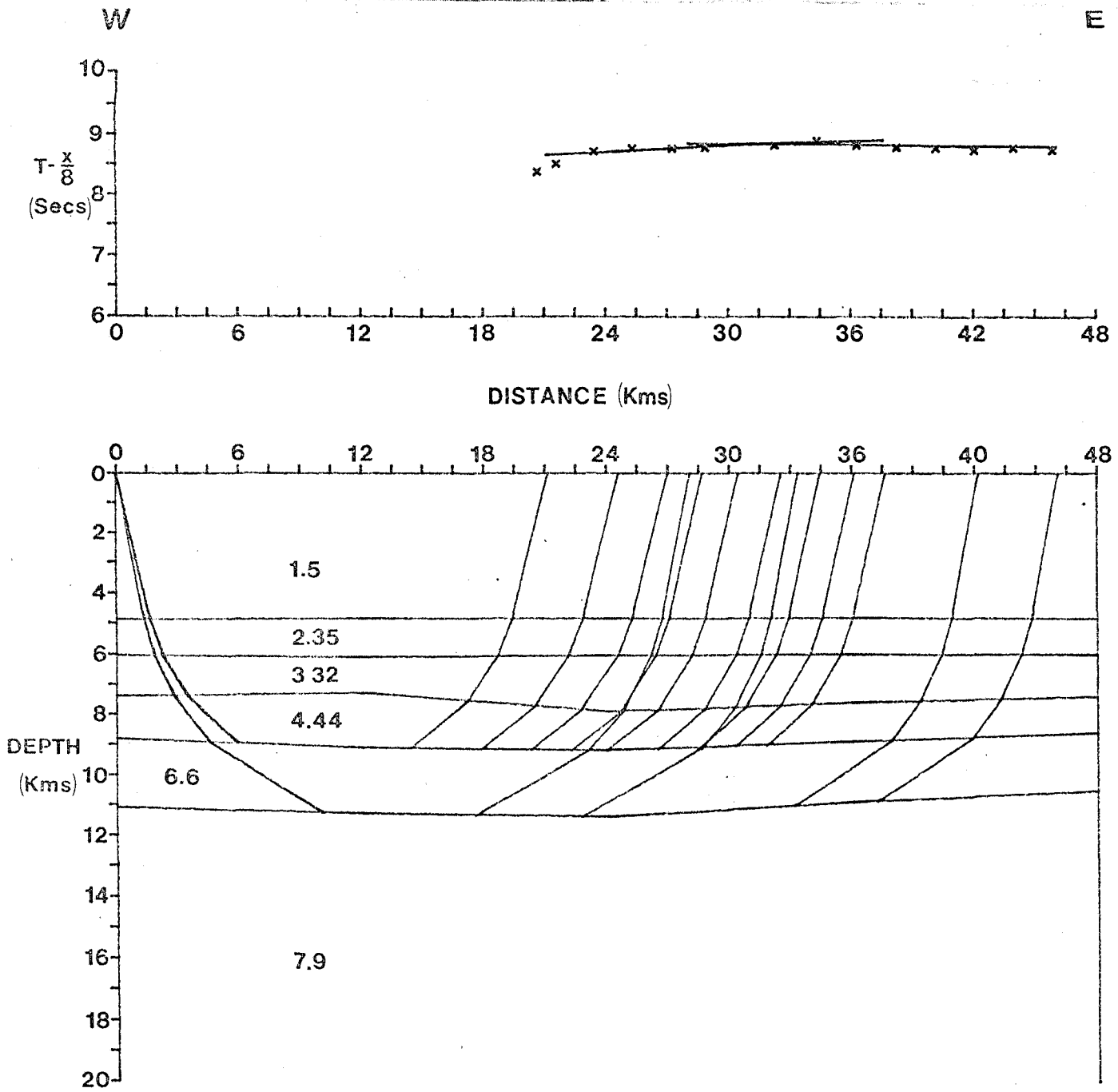

BISCAY 6702-4

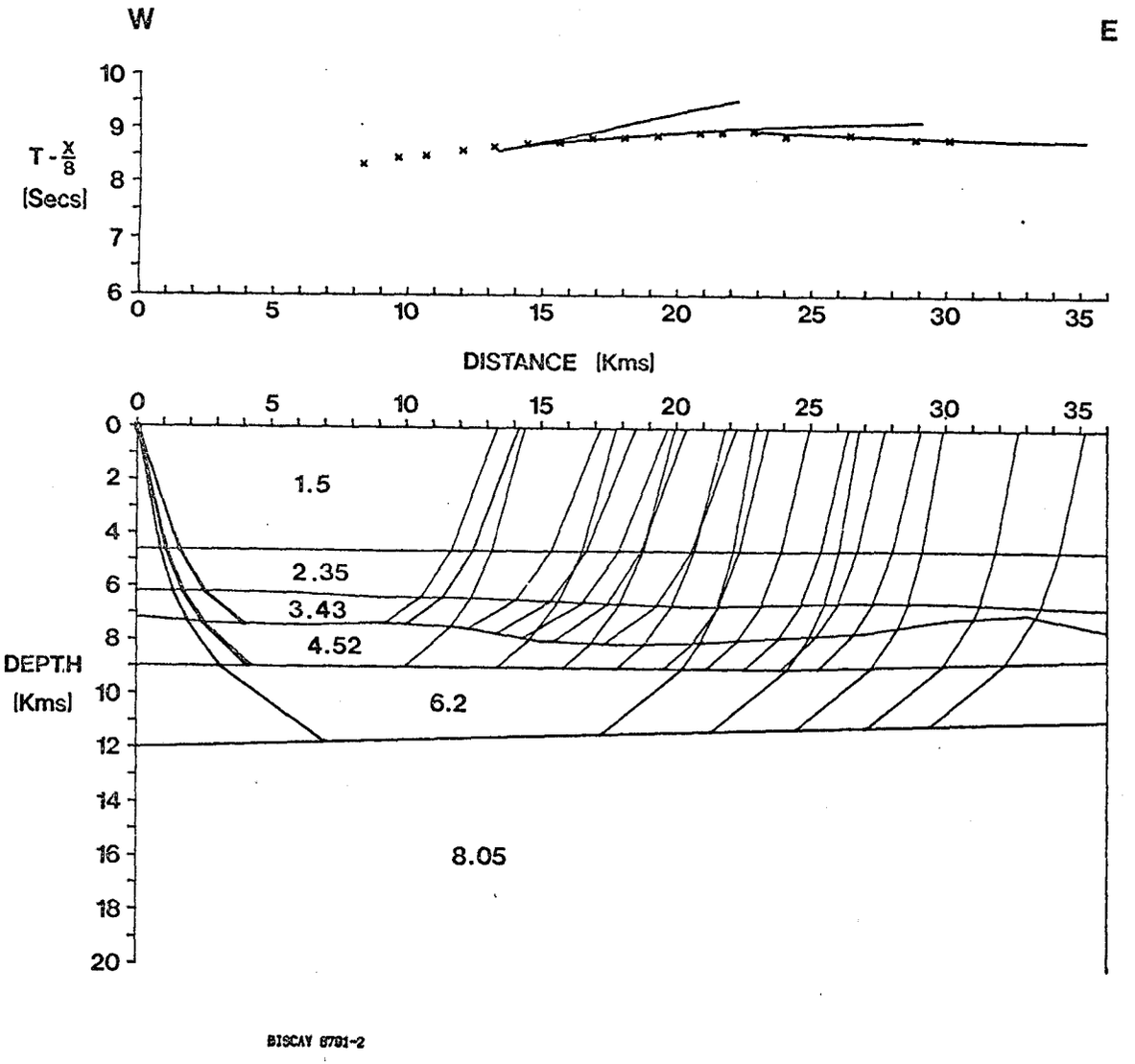

BISCAY 8701-2

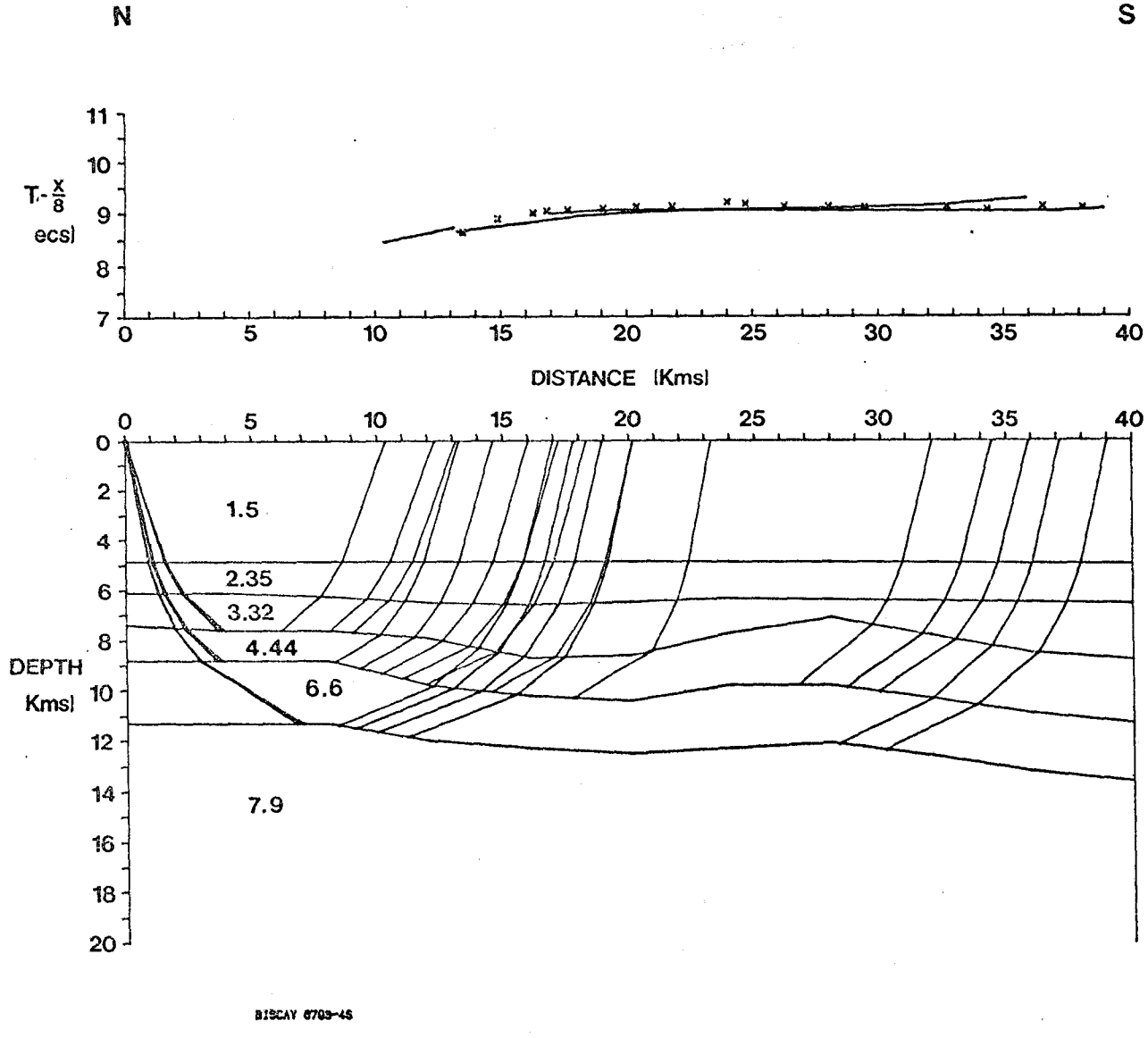
N
S
T.-X/8 ecs
DISTANCE (Kms)
DEPTH Kms
1.5
2.35
3.32
4.44
6.6
7.9
BISCAY 6709-46

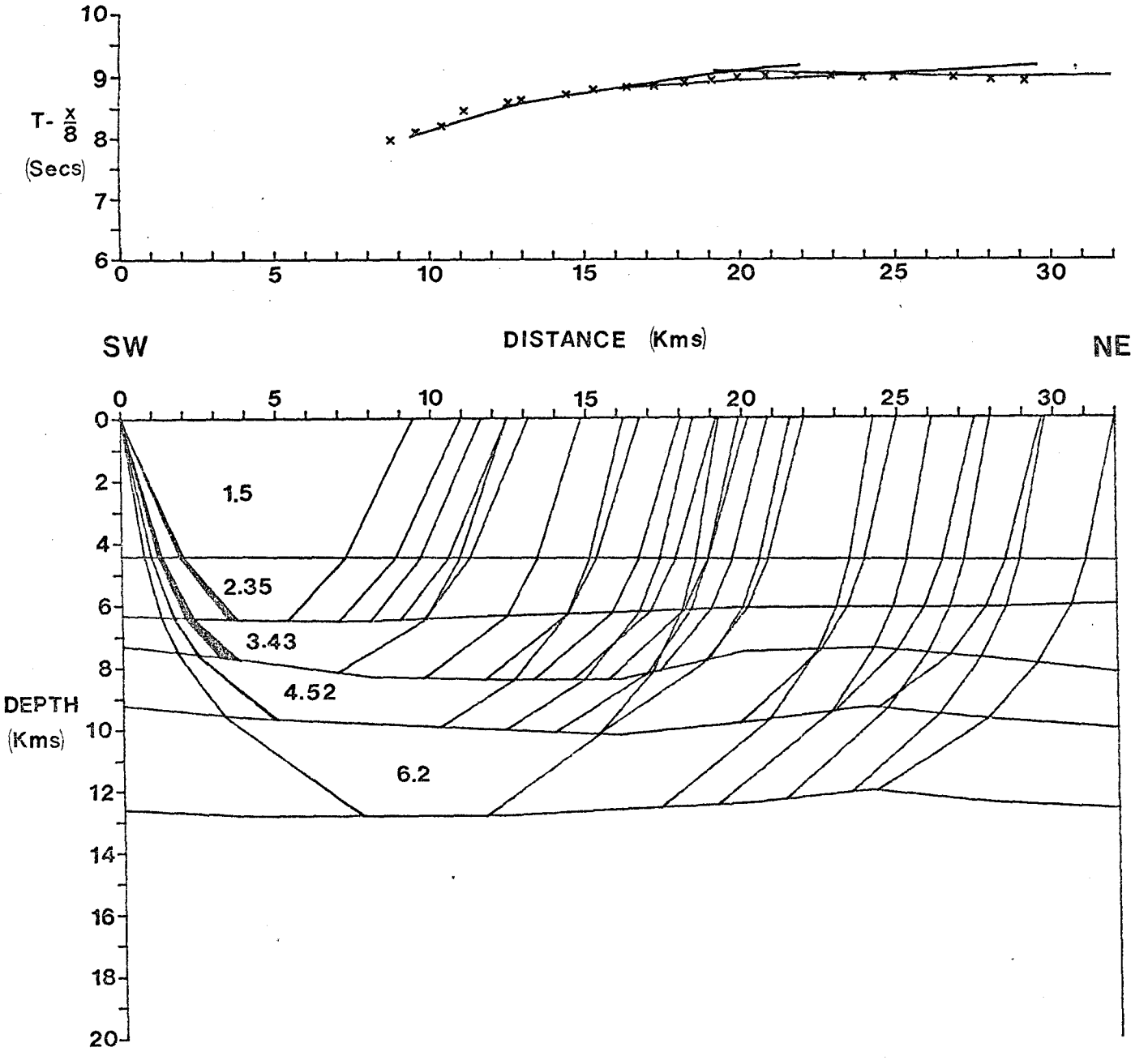

BISCAY 6793-2/S

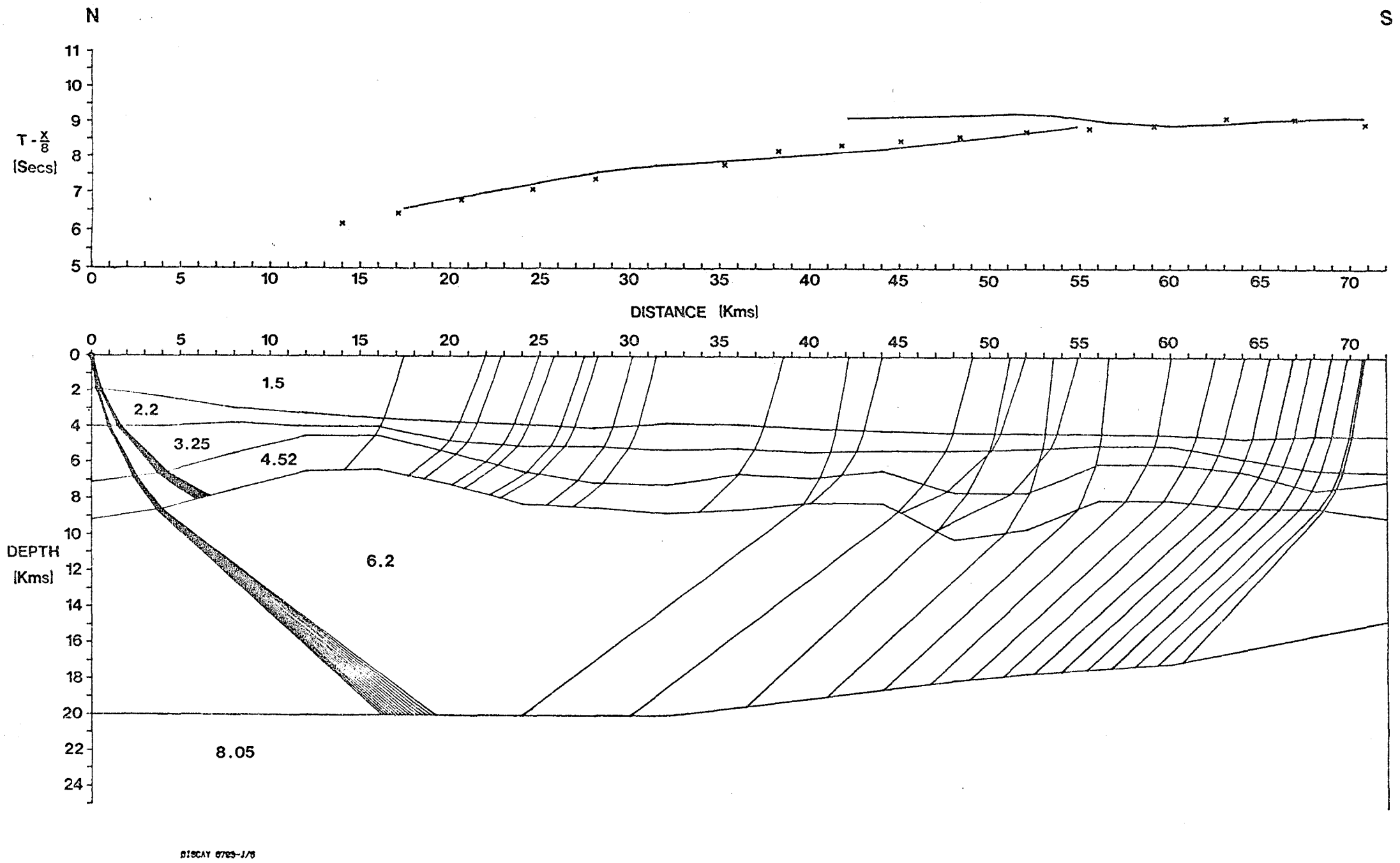

BISCAY 0703-J/6

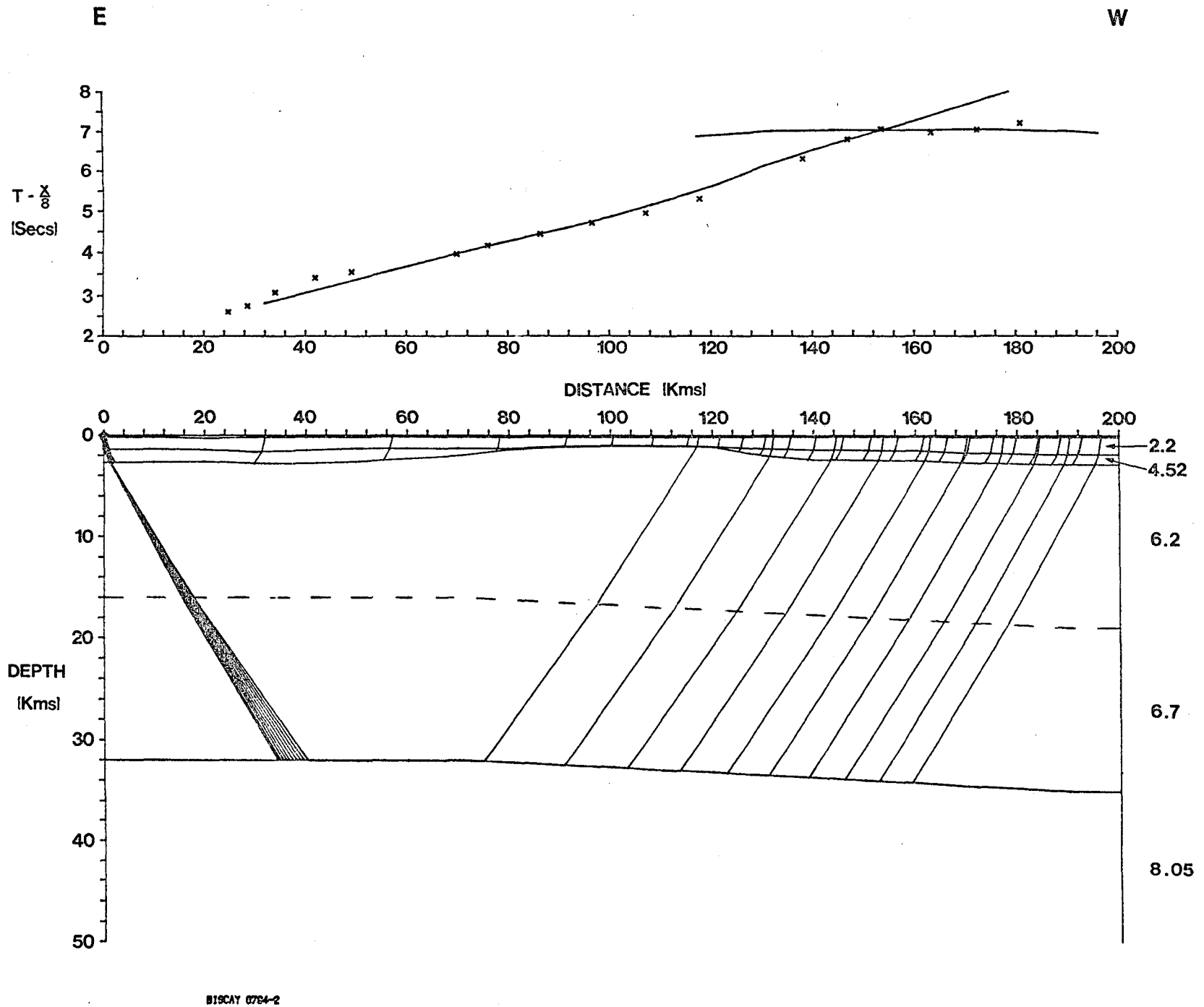
E
W
T - X/8
(Secs)
DISTANCE (Kms)
DEPTH
(Kms)
2.2
4.52
6.2
6.7
8.05
BISCAY 0784-2

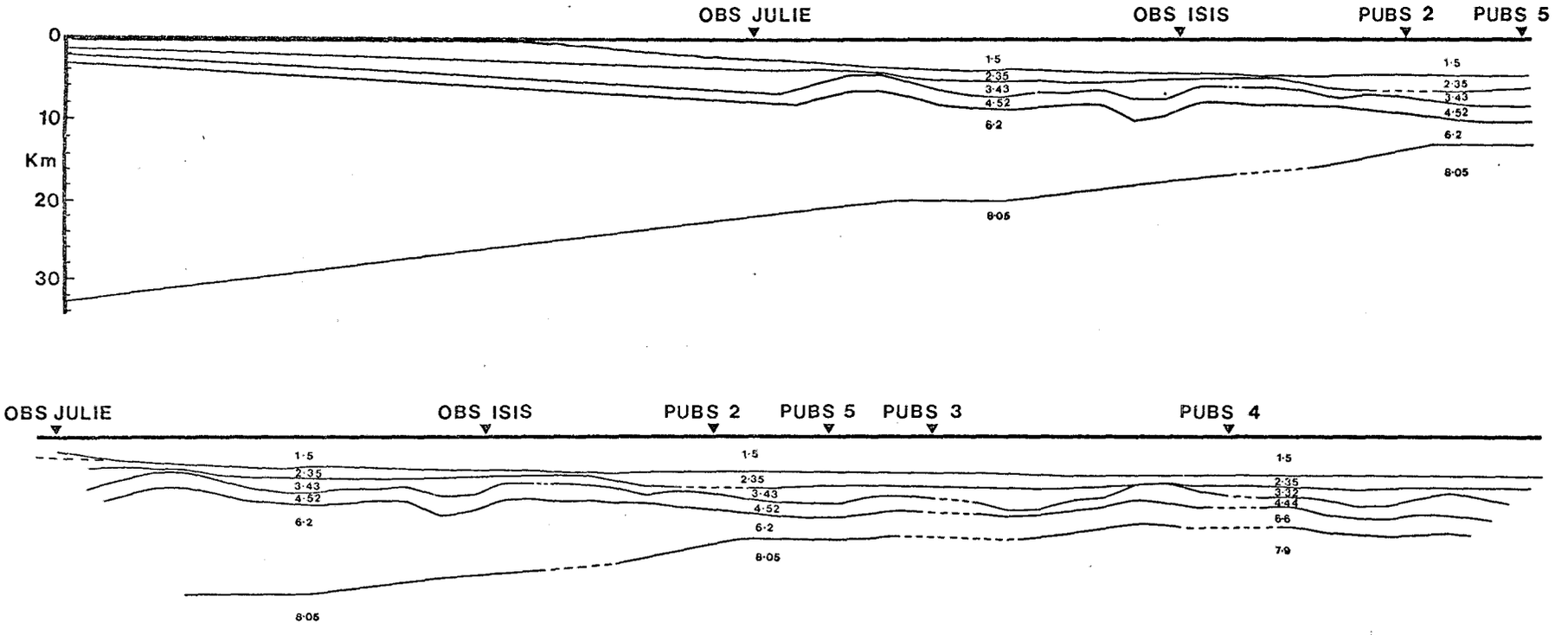

cont.

0 30

Kilometres

BISCAY LINE 3

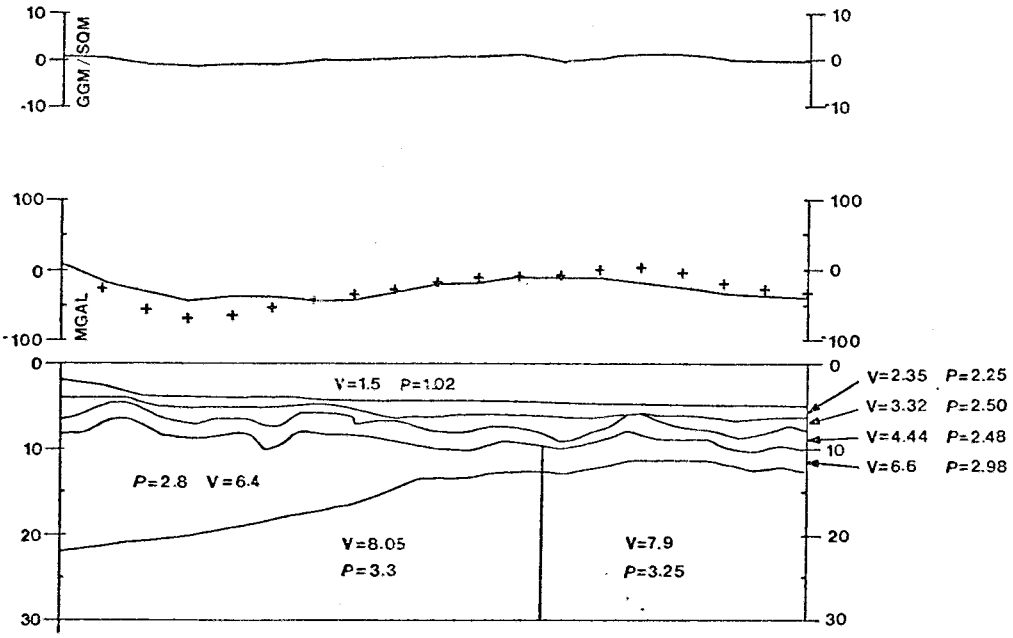

14A

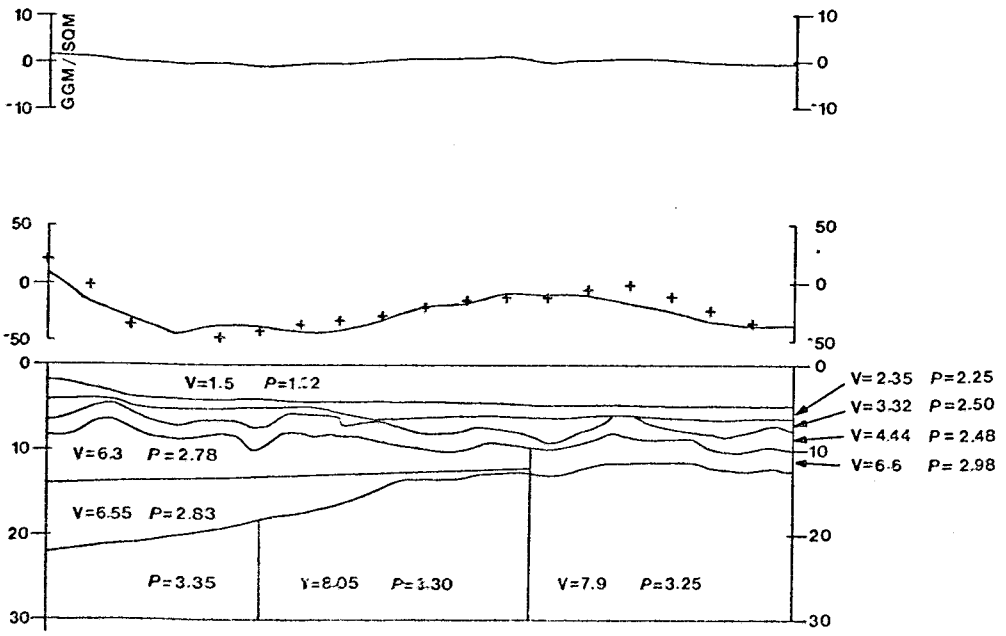

14B

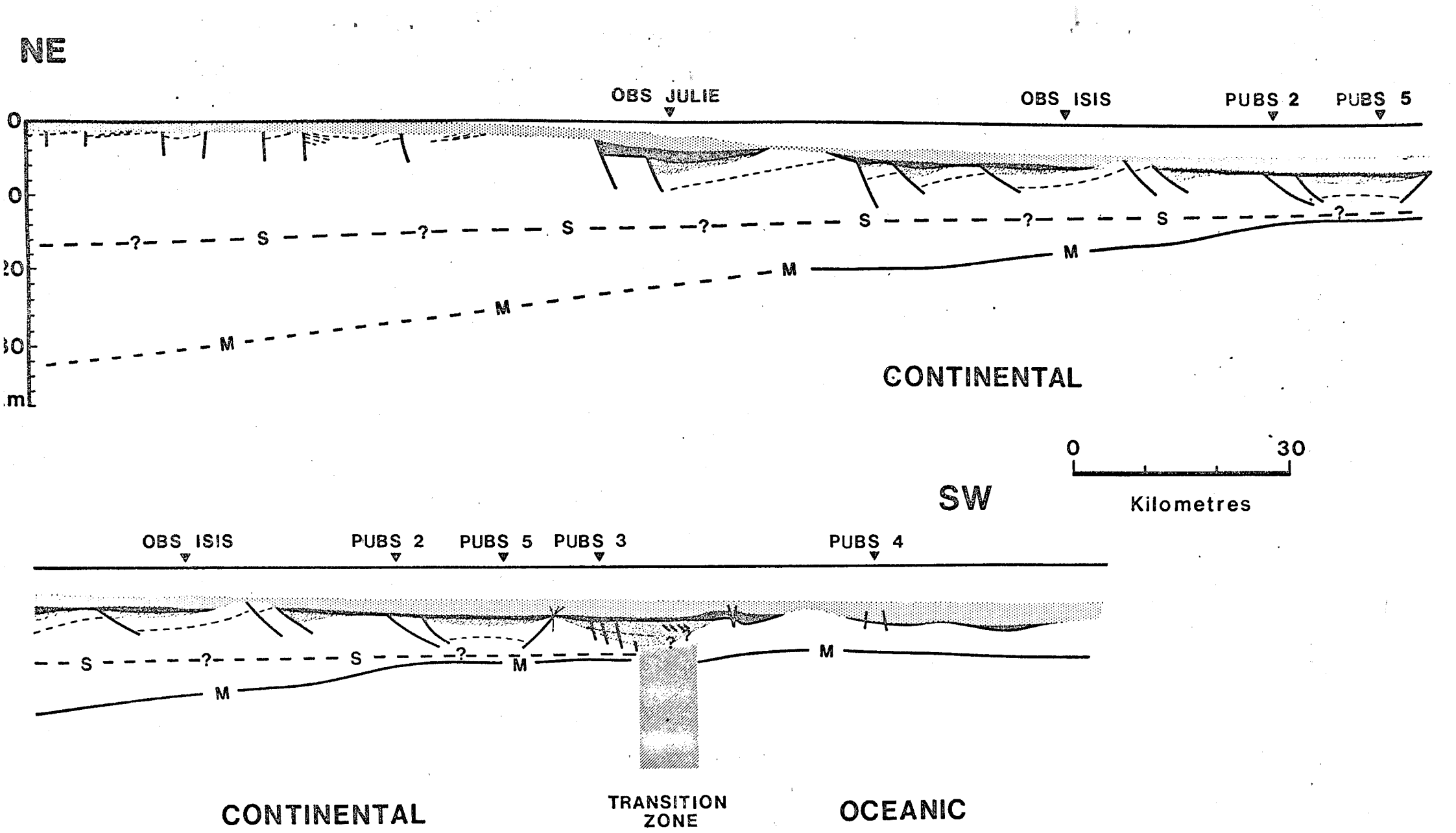
NE
OBS JULIE
OBS ISIS
PUBS 2
PUBS 5
0
0
20
30
km
S
M
CONTINENTAL
0
30
Kilometres
SW
OBS ISIS
PUBS 2
PUBS 5
PUBS 3
PUBS 4
CONTINENTAL
TRANSITION ZONE
OCEANIC